Outdoor Line-of-Sight Path Loss Modeling at 140 GHz

Brecht De Beelde, Emmeric Tanghe, David Plets, Wout Joseph
Ghent University - IMEC, Ghent, Belgium, Brecht.DeBeelde@UGent.be

***Abstract*—This paper presents outdoor radio channel measurements at 140 GHz using a spectrum analyzer-based channel sounder operational in the D-band, ranging from 110 to 170 GHz. We measure directional Line-of-Sight (LOS) path loss (PL) in a suburban environment for distances ranging from 2 m to 95 m, using an omnidirectional transmit antenna and directional receive antenna. Every 10 m, a full angular scan is performed by physically rotating the receive antenna in steps of 12°, which corresponds to the antenna's half-power beamwidth. A floating-intercept PL model is created, resulting in a fitted intercept PL_0 at 1 m of 80.7 dB, and PL exponent n 1.9. The azimuthal angular spread varies between 7° and 45°, with a mean angular spread of 19.7°.**

***Index Terms*—radio propagation modeling, D-band, channel sounder, outdoor, path loss**

I. Introduction

Fixed wireless access networks using the 60 GHz mm-wave frequency band have already proven to form a viable and cheaper alternative to the rollout and installation of fiber optic cables to provide broadband internet connectivity in residential areas [1]–[4]. With an increasing demand for high throughput wireless communication systems, wireless system engineers are already looking at sub-THz frequency bands where even higher bandwidths are available. This paper investigates the outdoor radio channel at center frequency 140 GHz.

Outdoor-to-indoor propagation at different mm-wave frequency bands is well investigated [5]–[12], but is less relevant at sub-THz frequencies because of the high building penetration losses. Outdoor channel modelling for fixed wireless access (FWA) and fifth generation (5G) telecommunication networks at mm-wave frequencies is discussed in multiple publications [13]–[16]. Channel models at D-band frequencies for indoor environments are provided in [17]–[23], but to the best of the authors' knowledge, no outdoor channel models exists at D-band frequencies.

In this paper, we present the design and validation of a D-band channel sounder, as well as outdoor measurements for distances up to 95 m. The novelty of this paper is not only the creation of an outdoor Line-of-Sight (LOS) path loss (PL) model at 140 GHz, we also discuss angular characteristics of the channel.

Section II presents the channel sounder design, measurement environment and path loss modeling methodology.

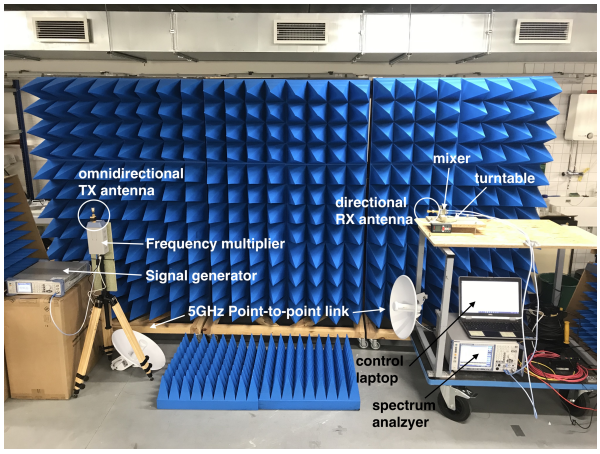

Fig. 1: Picture of the channel sounding setup.

In Section III, we present the validation of the sounder and provide the LOS PL model as well as angular spread analysis. Section IV concludes this paper.

II. Methodology

A. D-band channel sounder

For the outdoor channel measurement campaign, we use the D-band channel sounder from Fig. 1, which is operational in the D-band. A signal generator generates a radio frequency source from 9.167 to 14.167 GHz which is up-converted to D-band frequencies using a frequency multiplier. The continuous wave signal is transmitted via an omnidirectional D-band antenna with a gain of 3 dBi that is connected to the rectangular waveguide (WR-6) of the frequency multiplier. The vertically polarized transmit (TX) antenna has a return loss of 20 dB, an elevation half-power beamwidth (HPBW) of 45°, and has gain variations up to 2 dBi in a 40 GHz frequency band centered around 140 GHz. At the receiving side, a directional vertically polarized horn antenna with a gain of 23 dBi is used, connected to a harmonic mixer that down-converts the D-band signal to an intermediate frequency signal in frequency range 5 MHz to 3 GHz, using a local oscillator (LO) signal in frequency range 9 to 14 GHz. The receiving (RX) horn antenna has an azimuth HPBW of 12° and an elevation HPBW of 10°. Its gain variation over the full 60 GHz

band is 1 dBi and its return loss is 19.1 dB. The harmonic mixer has a conversion loss of 30 dB, and an uncertainty of 1.5 dB. A spectrum analyzer with a noise figure of 3 dB and displayed average noise level of -174 dBm/Hz, measures the power of the received signal. The cable for connecting the spectrum analyzer's LO port to the mixer has a loss of 1.7 dB in the LO frequency range. The maximum measurable path loss of this setup, calculated via (1), is 150 dB. In this equation, P_{TX} is the maximum transmit power of the frequency multiplier (6 dBm), G is the total antenna gain (26 dBi), L_{HM} is the mixer's conversion loss (30 dB), NL_{SA} is the noise level of the spectrum analyzer (-151 dBm, using a resolution bandwidth of 100 Hz), and NF_{SA} is the noise figure of the IF input of the spectrum analyzer (3 dB).

$$\begin{aligned} \mathrm{PL_{max}[dB]} = & \mathrm{P_{TX}[dBm]} + \mathrm{G[dBi]} - \mathrm{L_{HM}[dB]} \\ & - \mathrm{NL_{SA}[dBm]} - \mathrm{NF_{SA}[dB]} \end{aligned} \quad (1)$$

The signal generator and spectrum analzyer are connected to a laptop which is used to control the settings on both devices. For remote control of the signal generator, a point-to-point wireless link is used in the 5 GHz frequency band, therefore not influencing the measured channel.

We perform power measurements at frequency 140 GHz, with a frequency span of 1 MHz around the center frequency, using 501 frequency points and averaging factor 4. With the measurement bandwidth set to 100 Hz, the sweep duration of 1 measurement is 19 ms. From the measured received power we calculate PL via (2), with P_{TX} the transmit power, G the total antenna gain and $\mathrm{P_{RX}}$ the received power which takes into account the conversion loss calibration data of the harmonic mixer.

$$\mathrm{PL[dB]} = P_{TX}\mathrm{[dBm]} + G\mathrm{[dBi]} - \mathrm{P_{RX}[dBm]} \quad (2)$$

The frequency-dependent conversion loss of the mixer is obtained from calibration data, provided by the mixer's manufacturer. The frequency-dependent gain variations of the TX and RX antennas is fixed and taken into account by performing reference measurements. The uncertainty of the measurement setup is therefore only defined by the uncertainty of the harmonic mixer.

B. Measurement environment

We performed LOS measurements along seven tracks in a suburban outdoor environment, at a university campus in Ghent, Belgium. The location of the different tracks is shown in Fig. 2, in which fixed TX antenna locations are visualized by red circles, and the directional RX antenna moves away from the TX antenna in steps of 1 m, along the purple arrows. The antenna separations range from 2 to 95 m and both TX and RX antennas are placed at a height of 1.2 m. Both antennas are leveled and aligned, i.e., the RX antenna points towards the TX antenna.

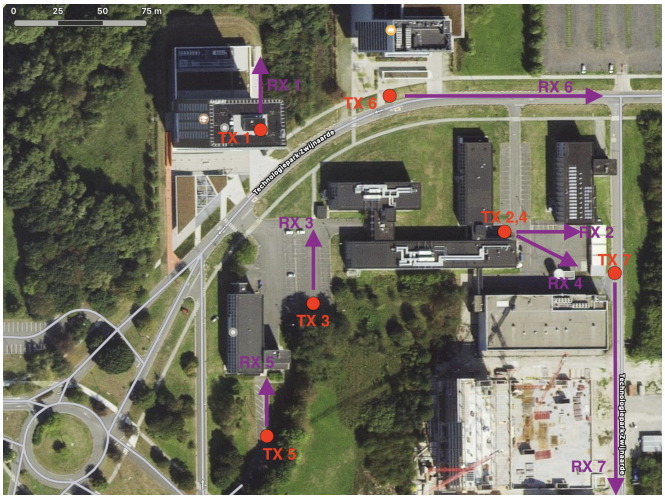

Fig. 2: Floorplan of university campus with different measurement tracks.

For distances up to 60 m, a full angular scan is performed every 10 m, by physically rotating the RX antenna over 360° in steps of 12°, which corresponds to the RX antenna's HPBW in the azimuth plane.

C. Line-of-Sight path loss modeling and angular channel characteristics

The measured LOS PL values of the seven tracks are fitted to the single-frequency floating-intercept (FI) model from (3), with d the distance in meters, $PL_0(f)$ the reference PL in dB at 1 m, $n(f)$ the PL exponent, and χ_σ the shadow fading term in dB, based on the 95% percentile of a zero-mean normal distribution with standard deviation σ.

$$\mathrm{PL_{FI,dB}}(d) = PL_0 + 10n\log_{10}(d/1\mathrm{m}) + \chi_\sigma \quad (3)$$

Based on the angular PL measurements, we analyze the angular characteristics of the outdoor channel. We calculate root-mean-square (RMS) angular spread (AS) via (4), with θ the angle of arrival in degrees and $\mathrm{P_{RX}}(\theta)$ the corresponding linear received power.

$$\mathrm{AS_{AoA}} = \sqrt{\frac{\sum_\theta \mathrm{P_{RX}}(\theta)\cdot\theta^2}{\sum_\theta \mathrm{P_{RX}}(\theta)} - \left(\frac{\sum_\theta \mathrm{P_{RX}}(\theta)\cdot\theta}{\sum_\theta \mathrm{P_{RX}}(\theta)}\right)^2} \quad (4)$$

III. Results

A. Channel sounder validation

The measurement system is validated over the full 60 GHz bandwidth of the D-band by performing reference measurements in the lab, where the walls and possible reflective objects are covered by absorbers, as can be seen in Fig. 1. For the validation measurements, the distance

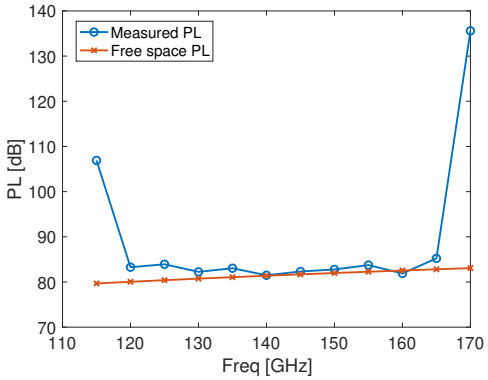

Fig. 3: Validation measurement results, with a distance of 2 m between the transmit and receiver antenna.

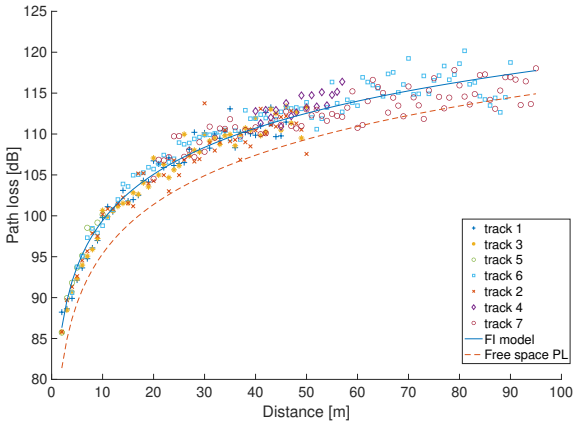

Fig. 4: Measured Line-of-Sight directional path loss in dB at frequency 140 GHz as a function of distance.

between the antennas was 2 m. From the measurement result, visualized in Fig. 3, we see a measurement error exceeding 25 dB for frequencies below 120 GHz and above 165 GHz. This error is caused by a deviation of the antenna gain of the TX antenna, which is reported in the antenna's datasheet. Therefore, the sounding setup is only validated for frequencies ranging from 120 to 165 GHz. The root-mean-squared-error (RMSE) between measured PL and FSPL is 1.96 dB, and is caused by the frequency-dependent gain variations of the TX and RX antennas, and the cable losses. When using shorter cables, with a loss of just 0.7 dB for frequencies ranging from 9 to 14 dB, i.e., the IF output of the harmonic mixer, the RMSE decreases to 1.50 dB. We use the validation measurement results as correction data, i.e., for every frequency we store the offset of measured PL and FSPL. This offset can be added to the measured received power during the channel measurements over the full band. At 140 GHz, the offset is 0 dB.

B. Line-of-Sight path loss

Fig. 4 shows the measured PL samples at 140 GHz for the different measurement tracks, as well as the fitted model evaluated at 140 GHz. Fitting the measured LOS PL samples to the FI model from (3) results in PL_0 = 80.7 dB and PL exponent n = 1.88. The RMSE between the fitted model and measured samples is 1.45 dB, which results in a shadow fading term χ_σ of 2.4 dB. The coefficient of determination of the fit R^2 is 0.955.

C. Angular spread

Fig. 5 shows the measured PL as a function of angle of arrival (AoA) and distance, for measurement track 1. Apart from the clear LOS path, some strong reflections are present, e.g., for AoA 50° at 10 m, and for AoA 156° at 30 m. Fig. 6 shows the angular spread values for the different distances and measurement tracks. Angular spread values range from 8° up to 43°, with a mean angular spread

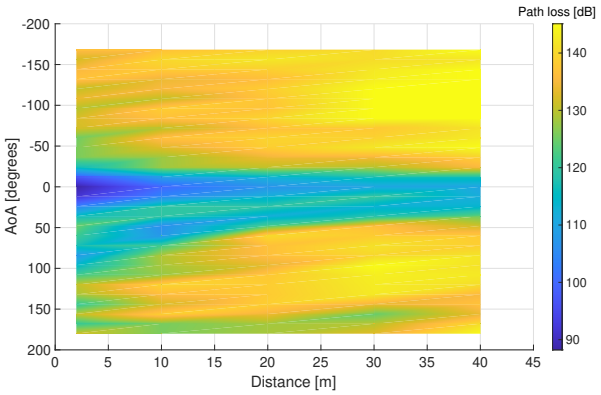

Fig. 5: Path loss at 140 GHz as a function of distance (x-axis) and angle of arrival (y-axis) for measurement track 1.

of 19.7°. For track 1, which is a track parallel to a 12-story building, at distance 6.2 m from the building's facade, the angular spread values are higher, due to the strong building reflection. For track 2, the angular spread clearly increases for higher distances, i.e., when the RX antenna is close to the building opposite to the TX antenna. Tracks 6 and 7 are in a more open environment, which explains the lower angular spread values. The low angular spread values for distances below 10 m are explained by the relatively larger path lengths of the reflected paths, compared to the small direct path distance.

IV. Conclusion

In this paper, we have investigated the outdoor radio channel at 140 GHz, using a spectrum analyzer-based channel sounder capable of characterizing the D-band for distances up to 100 m. After a validation of the channel

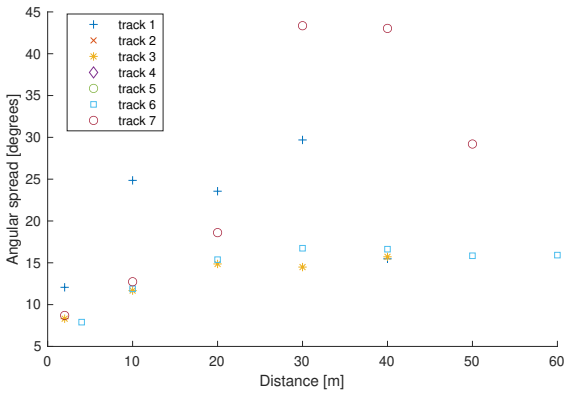

Fig. 6: Angular spread as a function of distance, for the different measurement tracks.

sounder in the lab, LOS measurements were performed in a suburban environment along multiple measurement tracks and fitted the measurement samples to a FI PL model. By performing a full angular scan at certain distances, an angular path loss model is obtained and angular spread values are calculated.

ACKNOWLEDGMENT

This work was executed within the imec AAA D-band channel modeling research project (D-BARC) and EOS project multi-service wireless network (MUSE-WINET). D-BARC received support from Flanders Innovation & Entrepreneurship.

REFERENCES

[1] K. Aldubaikhy, W. Wu, N. Zhang, N. Cheng, and X. Shen, "mmwave ieee 802.11ay for 5g fixed wireless access," *IEEE Wireless Communications*, vol. 27, no. 2, pp. 88–95, 2020.

[2] E.-M. Oproiu, I. Gimiga, and I. Marghescu, "5g fixed wireless access-mobile operator perspective," in *2018 International Conference on Communications (COMM)*, 2018, pp. 357–360.

[3] A. Nordrum, "Facebook pushes networking tech: The company's terragraph technology will soon be available in commercial gear - [news]," *IEEE Spectrum*, vol. 56, no. 4, pp. 8–9, 2019.

[4] A. Shkel, A. Mehrabani, and J. Kusuma, "A configurable 60ghz phased array platform for multi-link mmwave channel characterization," in *2021 IEEE International Conference on Communications Workshops (ICC Workshops)*, 2021, pp. 1–6.

[5] J. Lee, K.-W. Kim, M.-D. Kim, J.-J. Park, Y. K. Yoon, and Y. J. Chong, "Measurement-based millimeter-wave angular and delay dispersion characteristics of outdoor-to-indoor propagation for 5g millimeter-wave systems," *IEEE Access*, vol. 7, pp. 150 492–150 504, 2019.

[6] Y. C. Lee, S.-S. Oh, H. C. Lee, C. Woo Byeon, S. W. Park, I.-Y. Lee, J.-H. Lim, J.-I. Lee, and B.-L. Cho, "Measurements of window penetration loss and building entry loss from 3.5 to 24 ghz," in *2019 13th European Conference on Antennas and Propagation (EuCAP)*, 2019, pp. 1–4.

[7] R. Zhu, Y. E. Wang, Q. Xu, Y. Liu, and Y. D. Li, "Millimeter-wave to microwave mimo relays (m4r) for 5g building penetration communications," in *2018 IEEE Radio and Wireless Symposium (RWS)*, 2018, pp. 206–208.

[8] M. Khatun, C. Guo, D. Matolak, and H. Mehrpouyan, "Indoor and outdoor penetration loss measurements at 73 and 81 ghz," in *2019 IEEE Global Communications Conference (GLOBECOM)*, 2019, pp. 1–5.

[9] S. Y. Jun, D. Caudill, J. Chuang, P. B. Papazian, A. Bodi, C. Gentile, J. Senic, and N. Golmie, "Penetration loss at 60 ghz for indoor-to-indoor and outdoor-to-indoor mobile scenarios¡sup¿*¡/sup¿," in *2020 14th European Conference on Antennas and Propagation (EuCAP)*, 2020, pp. 1–5.

[10] A. B. Zekri, R. Ajgou, A. Chemsa, and S. Ghendir, "Analysis of outdoor to indoor penetration loss for mmwave channels," in *2020 1st International Conference on Communications, Control Systems and Signal Processing (CCSSP)*, 2020, pp. 74–79.

[11] J. Lee, "Cluster-based millimeter-wave outdoor-to-indoor propagation characteristics based on 32 ghz measurement analysis," *IEEE Antennas and Wireless Propagation Letters*, vol. 20, no. 1, pp. 73–77, 2021.

[12] Y. C. Lee, S.-S. Oh, C. W. Byeon, K. Aziding, and B.-L. Cho, "Impact of the window penetration loss on the building entry loss from 3.5 to 24 ghz," *IEEE Access*, pp. 1–1, 2021.

[13] M. K. Samimi, T. S. Rappaport, and G. R. MacCartney, "Probabilistic omnidirectional path loss models for millimeter-wave outdoor communications," *IEEE Wireless Communications Letters*, vol. 4, no. 4, pp. 357–360, 2015.

[14] X. Zhao, S. Li, Q. Wang, M. Wang, S. Sun, and W. Hong, "Channel measurements, modeling, simulation and validation at 32 ghz in outdoor microcells for 5g radio systems," *IEEE Access*, vol. 5, pp. 1062–1072, 2017.

[15] A. I. Sulyman, S. Buck, and T. J. Montano, "Effects of solar radio emissions on outdoor radio propagation at 38 ghz bands for d2d communications," *IEEE Antennas and Wireless Propagation Letters*, vol. 19, no. 5, pp. 741–745, 2020.

[16] M. Z. Aslam, Y. Corre, J. Belschner, G. S. Arockiaraj, and M. Jäger, "Analysis of 60-ghz in-street backhaul channel measurements and lidar ray-based simulations," in *2020 14th European Conference on Antennas and Propagation (EuCAP)*, 2020, pp. 1–5.

[17] S. Kim, W. T. Khan, A. Zajić, and J. Papapolymerou, "D-band channel measurements and characterization for indoor applications," *IEEE Transactions on Antennas and Propagation*, vol. 63, no. 7, pp. 3198–3207, 2015.

[18] C. Cheng, S. Kim, and A. Zajić, "Comparison of path loss models for indoor 30 ghz, 140 ghz, and 300 ghz channels," in *2017 11th European Conference on Antennas and Propagation (EUCAP)*, 2017, pp. 716–720.

[19] S. L. H. Nguyen, J. Järveläinen, A. Karttunen, K. Haneda, and J. Putkonen, "Comparing radio propagation channels between 28 and 140 ghz bands in a shopping mall," in *12th European Conference on Antennas and Propagation (EuCAP 2018)*, 2018, pp. 1–5.

[20] Y. Xing and T. S. Rappaport, "Propagation measurement system and approach at 140 ghz-moving to 6g and above 100 ghz," in *2018 IEEE Global Communications Conference (GLOBECOM)*, 2018, pp. 1–6.

[21] Y. Xing, O. Kanhere, S. Ju, and T. Rappaport, "Indoor wireless channel properties at millimeter wave and sub-terahertz frequencies," in *2019 IEEE Global Communications Conference (GLOBECOM)*, 12 2019, pp. 1–6.

[22] L. Pometcu and R. D'Errico, "Channel model characteristics in d-band for nlos indoor scenarios," in *2019 13th European Conference on Antennas and Propagation (EuCAP)*, 2019, pp. 1–4.

[23] B.-E. Olsson, C. Larsson, M. N. Johansson, and S. L. H. Nguyen, "Radio propagation in an office environment at 140 ghz and 28 ghz," in *2021 15th European Conference on Antennas and Propagation (EuCAP)*, 2021, pp. 1–5.